RESEARCH PAPER

Annexin-A1 deficiency exacerbates pathological remodelling of the mesenteric vasculature in insulin-resistant, but not insulin-deficient, mice

Maria Jelinic[1,2] | Nicola Kahlberg[1] | Chen Huei Leo[1,3] | Hooi Hooi Ng[1,5] | Sarah Rosli[4] | Minh Deo[4] | Mandy Li[4] | Siobhan Finlayson[4] | Jesse Walsh[4] | Laura J. Parry[1] | Rebecca H. Ritchie[4,6,7] | Cheng Xue Qin[4,6,7]

[1]School of BioSciences, University of Melbourne, Melbourne, VIC, Australia

[2]Department of Physiology, Anatomy and Microbiology, La Trobe University, Melbourne, VIC, Australia

[3]Science, Math and Technology, Singapore University of Technology and Design, Singapore

[4]Heart Failure Pharmacology, Baker Heart and Diabetes Institute, Melbourne, VIC, Australia

[5]Department of Human and Molecular Genetics, Herbert Wertheim College of Medicine, Florida International University, Miami, Florida

[6]Department of Diabetes, Central Clinical School, Monash University, Melbourne, VIC, Australia

[7]Department of Pharmacology and Therapeutics, University of Melbourne, Melbourne, VIC, Australia

Correspondence
Dr Cheng Xue Qin, PhD, Adjunct Research Fellow (University of Melbourne), and Prof. Rebecca Ritchie, PhD, FCSANZ, FAHA, NHMRC Senior Research Fellow, Adjunct Professor (Monash University), Heart Failure Pharmacology, Baker Heart and Diabetes Institute, 75 Commercial Rd, Melbourne 3004 Australia.
Email: chengxuehelena.qin@baker.edu.au; rebecca.ritchie@monash.edu.au

Background and purpose: Arterial stiffness, a characteristic feature of diabetes, increases the risk of cardiovascular complications. Potential mechanisms that promote arterial stiffness in diabetes include oxidative stress, glycation and inflammation. The anti-inflammatory protein annexin-A1 has cardioprotective properties, particularly in the context of ischaemia. However, the role of endogenous annexin-A1 in the vasculature in both normal physiology and pathophysiology remains largely unknown. Hence, this study investigated the role of endogenous annexin-A1 in diabetes-induced remodelling of mouse mesenteric vasculature.

Experimental approach: Insulin-resistance was induced in male mice (*AnxA1*^{+/+} and *AnxA1*^{-/-}) with the combination of streptozotocin (55mg/kg i.p. x 3 days) with high fat diet (42% energy from fat) or citrate vehicle with normal chow diet (20-weeks). Insulin-deficiency was induced in a separate cohort of mice using a higher total streptozocin dose (55mg/kg i.p. x 5 days) on chow diet (16-weeks). At study endpoint, mesenteric artery passive mechanics were assessed by pressure myography.

Key results: Insulin-resistance induced significant outward remodelling but had no impact on passive stiffness. Interestingly, vascular stiffness was significantly increased in *AnxA1*^{-/-} mice when subjected to insulin-resistance. In contrast, insulin-deficiency induced outward remodelling and increased volume compliance in mesenteric arteries, regardless of genotype. In addition, the annexin-A1 / formyl peptide receptor axis is upregulated in both insulin-resistant and insulin-deficient mice.

Conclusion and implications: Our study provided the first evidence that endogenous AnxA1 may play an important vasoprotective role in the context of insulin-resistance. AnxA1-based therapies may provide additional benefits over traditional anti-inflammatory strategies for reducing vascular injury in diabetes.

1 | INTRODUCTION

The passive mechanical properties of the vascular wall play a vital role in assisting normal function of the cardiovascular system. When vessels stiffen, the ability of the vascular wall to recoil is reduced, increasing pulse pressure, which in turn damages the smaller peripheral vessels (Henry et al., 2003; Martinez-Lemus, Hill, & Meininger, 2009). Vascular stiffening is a hallmark of many cardiovascular diseases, where diabetes mellitus is a major risk factor (Henry et al., 2003; Stehouwer, Henry, & Ferreira, 2008; Zieman, Melenovsky, & Kass, 2005). In addition, vascular stiffness is a critical factor for the initial development of vascular complications in diabetes (Prenner et al., 2015; Wilkinson, Westerbacka, Yki-Jarvinen, & Cockcroft, 2001). Thus, developing novel strategies to target vascular stiffening offer significant therapeutic potential for the treatment of the vascular complications of diabetes.

There are three common types of diabetes—Type 1, Type 2, and gestational diabetes. The most common type of diabetes is Type 2 diabetes (T2D), often considered a lifestyle disease. It is commonly associated with a combination of factors including increased bodyweight, smoking, excessive alcohol intake, and physical inactivity (Huynh, Bernardo, McMullen, & Ritchie, 2014; Zimmet, Alberti, & Shaw, 2001). The sustained release of insulin from the pancreas in this context occurs in order to maintain homeostasis with elevated blood glucose concentrations, ultimately leading to insulin resistance (Zimmet et al., 2001). In contrast, Type 1 diabetes (T1D) is an autoimmune disease characterised by the gradual destruction of pancreatic beta-islet cells, resulting in insulin deficiency (Raskin et al., 2010; Zimmet et al., 2001). The remodelling of the resistance vasculature (e.g., mesenteric arteries) in diabetes has been largely studied in rodent models of T1D. The general consensus from these studies is that diabetes induces outward hypertrophic remodelling in mesenteric arteries (Crijns, Wolffenbuttel, De Mey, & Boudier, 1999; Souza-Smith et al., 2011), mostly attributed to increased oxidative stress and inflammatory response (Huynh et al., 2014; Zimmet et al., 2001). We recently confirmed that streptozotocin (STZ)-induced T1D elicits outward hypertrophic remodelling and increased stiffness in rats with moderate (∼20-mM blood glucose) or severe hyperglycaemia (∼30-mM blood glucose; Kahlberg et al., 2016). However, other reports suggest that diabetes increased circumferential stiffness only in the femoral artery, but not in mesenteric arteries (Wigg et al., 2004). In most studies, the effects of diabetes on vascular remodelling have focused in T1D models. Little is known regarding the effects of T2D on resistance vascular remodelling despite 90% of diabetic patients exhibiting T2D (Huynh et al., 2014; Zimmet et al., 2001). Thus, further work is warranted to better understand the relative effects of insulin resistance relative to those of insulin deficiency, on vascular remodelling, particularly in resistance vessels.

Diabetes is a low-grade, chronic inflammatory disorder (Devaraj, Dasu, & Jialal, 2010; Huynh et al., 2014). Circulating levels of inflammatory markers (such as C-reactive protein and pro-inflammatory cytokines) are increased in diabetic patients, as is

What is already known
- The endogenous anti-inflammatory protein annexin-A1 is cardioprotective against acute severe ischaemic insults.

What does this study add
- The role of endogenous annexin-A1 in diabetes-induced remodelling in mouse mesenteric vasculature.

What is the clinical significance
- Annexin-A1-based strategies may represent a novel therapy to reduce vascular damage in patients with insulin-resistance.

monocyte adhesion to the endothelium (Hanley et al., 2004; Schalkwijk et al., 1999). Targeting this vascular inflammation, and the resolution of inflammatory pathways, may reduce adverse vascular remodelling in diabetes. Annexin-A1 (AnxA1) is a naturally occurring anti-inflammatory protein that belongs to the annexin superfamily (Perretti & Dalli, 2009; Qin et al., 2015). It is an important second messenger for glucocorticoids and mediates many of their anti-inflammatory actions (Perretti & D'Acquisto, 2009). Mice deficient in AnxA1 exhibit an exaggerated response to many inflammatory disorders, including pulmonary fibrosis (Damazo et al., 2011), rheumatoid arthritis (Yang et al., 2004), stroke (Gavins, Dalli, Flower, Granger, & Perretti, 2007), and endotoxemia (Damazo et al., 2005; Qin et al., 2015). This is consistent with our previous observations that exogenous AnxA1 preserves myocardial function in ischaemia–reperfusion injury in vitro (Qin et al., 2013; Ritchie, Gordon, Woodman, Cao, & Dusting, 2005; Ritchie, Sun, Bilszta, Gulluyan, & Dusting, 2003).

AnxA1 is expressed in endothelial cells and vascular smooth muscle cells in the vasculature (Pan et al., 2016; Paravicini, Yogi, Mazur, & Touyz, 2009), where it exhibits anti-inflammatory properties (Pan et al., 2016). Levels of AnxA1 are elevated in individuals with T1D, and deficiency in AnxA1 exhibits a more severe diabetic phenotype in the heart and kidney, compared to diabetic wild-type mice (Purvis et al., 2018). In addition, the levels of AnxA1 are also elevated in patients with T2D, and AnxA1 deficiency mice fed a high-fat diet (HFD) exhibt a more severe diabetic phenotype, including dyslipidaemia, insulin resistance (Purvis et al., 2019). However, the effects of AnxA1 deficiency on arterial wall stiffness have not been studied. The aim of the current study was to investigate the effects of AnxA1 deficiency on vascular remodelling and stiffness, in both insulin-resistant and insulin-deficient mice. We hypothesised that insulin resistance and deficiency would exhibit different adverse remodelling in the mesenteric vasculature and that this would be exacerbated in $AnxA1^{-/-}$ mice.

2 | METHODS

2.1 | Animals

All animal care and experimental procedures complied with the National Health and Medical Research Council (NHMRC) of Australia code of practice for the care and use of animals for scientific purposes, ARRIVE guidelines, and Directive 2010/63/EU of the European Parliament in the protection of animal used for scientific purpose. Animal care and experimental protocols were approved by the Alfred Medical Research and Educational Precinct (AMREP) Animal Ethics Committee (E/1535/2013/B). Animal studies are reported in compliance with the ARRIVE guidelines (Kilkenny, Browne, Cuthill, Emerson, & Altman et al., 2010) and with the recommendations made by the *British Journal of Pharmacology*.

Male $AnxA1^{+/+}$ wild-type and $AnxA1^{-/-}$ mice (on a C57BL/6 background; Hannon et al., 2003) were bred and housed in individually ventilated cages (maximum of six non-diabetic or four diabetic mice per cage) at the AMREP Animal Centre and maintained under a 12-hr light/dark cycle, with food and water provided ad libitum for study in two distinct models of diabetes, insulin deficiency and insulin resistance. Regular welfare-related assessments were carried out throughout the study. Specifically, mice were monitored daily. Animals identified as unwell were placed on an Animal Care form and any pain or ailments were treated accordingly. Animals that responded to treatment and fully recovered were allowed to continue in the study. Animals not responding at all to treatment or showing signs of ongoing deterioration within 24 hr were removed from the remainder of the study and humanely killed.

Insulin resistance was induced in 6-week-old male $AnxA1^{-/-}$ and $AnxA1^{+/+}$ mice. Animals were randomly assigned to receive three consecutive daily i.p. injections of STZ (55 mg·kg^{-1} body weight, in 0.1-M citrate vehicle, pH 4.5; Sigma-Aldrich, St Louis, MO, USA) with concomitant HFD (SF04-001, 42% energy intake from lipids, Specialty Feeds, WA). The corresponding sham animals received three consecutive daily i.p. injections of citrate vehicle with concomitant normal chow diet. Blood glucose levels and body weight were monitored every 2 weeks for a period of 20 weeks. Mice allocated to low-dose STZ/HFD that exhibited blood glucose levels of 12- to 20-mM were considered to be insulin resistant, whereas mice that were fed a normal diet and given citrate vehicle injections were considered as non-diabetic sham controls and presented with blood glucose levels <12 mM. Blood glucose and body weight were monitored fortnightly using a handheld glucometer (ACCU-CHEK Advantage, Roche, Basel, Switzerland) until endpoint (20 weeks of insulin resistance or sham). Glucose tolerance testing was conducted in 5-hr fasted mice in vivo 1 week prior to cull. After a baseline glucose reading, 25% glucose solution (Baxter, Viaflex®, i.p.) was injected as a single bolus at the beginning of each i.p. glucose tolerance experiment, after which blood glucose measurements were obtained via tail vein bleeds. Blood glucose was measured at baseline (0 min), 15, 30, 45, 60, 90, and 120 min after injection of glucose.

Insulin-deficient T1D was induced in a separate cohort of mice, using a higher total STZ dose, as previously described (Ng et al., 2017; Ritchie et al., 2012). Briefly, 6-week-old male $AnxA1^{-/-}$ and $AnxA1^{+/+}$ mice were randomly assigned to receive five consecutive daily i.p. injections of STZ, to induce insulin deficiency (55 mg·kg^{-1} body weight per day, in 0.1-M citrate vehicle, pH 4.5; Sigma-Aldrich, St Louis, MO, USA) or five consecutive daily i.p. injections of citrate vehicle of equivalent volume (sham group), following an overnight fast. Both T1D and sham mice received normal chow diet. Insulin deficiency was confirmed in mice if blood glucose was >25 mM at study endpoint. Blood glucose and body weight were monitored fortnightly using a handheld glucometer until endpoint (16 weeks of insulin deficiency or sham).

2.2 | In vivo analyses at study endpoint

Arterial BPs and heart rate were examined at experimental endpoint (16 and 20 weeks in the insulin-resistant and insulin-deficient studies, respectively). This was determined via catheterisation in anaesthetised mice (ketamine/xylazine/atropine: 100/10/1.2 mg·kg^{-1} i.p.) using a 1.4 Fr Millar MICRO-TIP pressure catheter and a Powerlab System (AD Instruments, Bella Vista, NSW, Australia) as described previously (Ritchie et al., 2012). A Cobas HbA1c analyser (Roche, Sydney, NSW, Australia) was used to determine HbA1c levels. Plasma insulin levels were determined using a mouse insulin ELISA (cat# 80-INSMSU-E01; ALPCO, Boston, USA), according to the manufacturer's instructions. Multiple ELISA plates were required to assess all the plasma samples in the study. To limit plate-to-plate variation, data were expressed as mean fold change relative to the within-plate control group ($AnxA1^{+/+}$ sham).

2.3 | Passive mechanical wall properties ex vivo

Following catheterisation, a section of the mesenteric arcade was immediately placed in an ice-cold Krebs' bicarbonate solution (mM: NaCl 120, KCl 5, MgSO$_4$ 1.2, KH$_2$PO$_4$ 1.2, NaHCO$_3$ 25, D-glucose 11.1, and CaCl$_2$ 2.5). First-order mesenteric arteries were cleared of fat and connective tissue and leak-free segments were mounted on the cannula of a pressure myograph (Living Systems Instrumentation, Burlington, VT, USA) and placed in a Ca^{2+}-free physiological saline solution (mM: NaCl 14.9, KCl 4.7, NaHCO$_3$ 4.7, KH$_2$PO$_4$ 1.2, MgSO$_4$ 1.7, glucose 5, HEPES 10, and EGTA 2). The lumen was gently flushed with physiological saline solution to remove any remaining blood, and the distal end of the artery was occluded and left free to allow it to lengthen passively with pressure.

Arteries were incubated at 37°C for 20 min prior to determination of vessel wall parameters. These included vessel length, outer diameter (OD), and wall thickness, in 10-mmHg increments from 5 to 120 mmHg. Parameters were obtained using a Nikon

Eclipse TS100 inverted microscope with a Hitachi KP-M3AN CCD camera attached. This was projected onto a monitor, and parameters were measured manually using a ruler and then converted into microns using a conversion factor (calculated from measurements made using a graticule) measured on a screen. Inner diameter (ID), wall stress, and wall strain were calculated as described previously (Jelinic et al., 2014). Wall cross-sectional area was calculated as $[(\pi \times OD^2)/4] - [(\pi \times ID^2)/4]$. Volume distensibility was calculated as Δ volume/([Δ cross-sectional area $\times$ length] $\times$ Δ Pressure), where cross-sectional area was calculated as $[(\pi \times ID^2)/4]$ (Leo, Jelinic, Gooi, Tare, & Parry, 2014). Volume compliance was calculated for each pressure increment using the following calculation: volume compliance = (Δ volume)/(Δ pressure), where Δ volume = (Δ cross-sectional area) $\times$ (Δ length), and cross sectional area = $(\pi \times ID^2)/4$ (Jelinic, Conrad, Tare, & Parry, 2015). The % change in length with pressure was calculated using the following equation: % length = [(value at pressure)/(value at baseline)] $\times$ 100 (Jelinic et al., 2015).

2.4 | Quantitative PCR

To further study the effects of AnxA1 on endothelium-dependent vasodilation and smooth muscle constriction, the expression of genes of interest, for example, *mouse formyl peptide receptor* 1 (*mFpr1*), *mFpr2*, *mAnxA1*, and *mMcp-1*, was analysed. Frozen blood vessels (each *n* number consisted of first- and second-order mesenteric arteries from one to two mice) were placed in pre-chilled Wig-L-Bug® capsules with a silver ball bearing and pulverised in a Digital Wig-L-Bug® amalgamator (Dentsply-Rinn, Elgin, IL, USA). Pulverised tissues were resuspended in 1-ml TriReagent (Ambion Inc., Scoresbury, VIC, Australia), and total RNA was then extracted as described previously (Jelinic et al., 2017). RNA pellets were resuspended in 12-µl RNA Secure™ (Ambion). Quality and quantity of RNA were analysed using the NanoDrop ND1000 Spectrophotometer (Thermo Fischer Scientific Australia Pty Ltd, Scoresby, VIC, Australia) with $A_{260}:A_{280}$ ratios >1.8 indicating sufficient quality for quantitative real-time PCR (qPCR) analysis. First-strand cDNA synthesis was performed using the RT^2 First Strand Kit (QIAGEN, Maryland, USA) as per instructions using 0.5 µg of total RNA per reaction. The qPCR analysis of genes of interest was performed using RT^2 Profiler™ Custom PCR Array for Mouse (QIAGEN) as per kit instructions for the AB Applied Biosystems 7500 Real-Time PCR System (Life Technologies, Mulgrave, VIC, Australia) in 20-µl volume reactions. β-actin (*Actb2*), β-2 microglobulin (*B2m*), and GAPDH (*Gapdh*) were the reference genes; however, there were significant differences between groups for all of these genes, and thus, for each diabetic setting, the control group (*AnxA1*$^{+/+}$ sham) was used as the internal calibrator, and this was subtracted from the mean gene of interest triplicate CT value [Ratio (test/calibrator) = 2ΔCT, where ΔCT = CT (calibrator) − CT (test)] as has been described previously (Marshall, Ng, Unemori, Girling, & Parry, 2016). These "normalised"

data (ΔCT) were presented as fold induction relative to the control group (*AnxA1*$^{+/+}$ sham).

2.5 | Immunohistochemistry

The antibody-based procedures used comply with the recommendations made by the *British Journal of Pharmacology* (Alexander et al., 2018). Mouse mesenteric arteries (*AnxA1*$^{+/+}$ mice) were fixed in neutral-buffered formalin, embedded in paraffin (Alfred Pathology Service, Melbourne, VIC, Australia), and then sectioned at 4 µm. Sections were deparaffinised and rinsed, and antigen retrieval was performed by incubating the slides for 20 min at 95°C in 0.01% citrate buffer. Sections were blocked in 5% NGS in 0.01% PBS/Tween 20 for 1 hr. To detect the expression of FPR1 and FPR2 in the vessel, sections were then incubated overnight at 4°C with either FPR1 primary antibody (1:100 in 5% NGS and 0.01% PBS-T, Biorbyt Cat# orb13410, RRID:AB_10752393, Cambridge, UK) or FPR2 primary antibody (1:100 in 5% NGS and 0.01% PBS-T, sc-66901, Bioss Cat# bs-3654R, RRID:AB_10858084, Texas, USA). Representative images were photographed as described previously (Qin et al., 2019). Positive FPR1 or FPR2 stained brown and grading was as follows: score 0, negative stain; score 1, very weak; score 2, weak; score 3, moderate; score 4, intense; score 5, very intense. Three to five sections were assessed per mouse, and five to seven mice were analysed per group; all assessments were made blindly, i.e., without knowledge of treatments.

2.6 | Data and statistical analysis

The data and statistical analysis comply with the recommendations of the *British Journal of Pharmacology* on experimental design and analysis in pharmacology (Curtis et al., 2018). All data are expressed as mean ± SEM. All figure formatting and statistical analyses were undertaken using Prism version 5.0 (GraphPad Software, San Diego, CA, USA). Certain experiments were undertaken in duplicate (ELISA) to ensure the reliability of single values. Data analysis and data presentation from these experiments used the single values obtained from the mean of the technical replicates used. "*n*" refers to number of animals (independent values), not replicates or independent experiments. For all experimental protocols, sample sizes were based on the number required to provide >80% power to detect an effect size of 20% at *P* < .05. All analyses were performed blindly whereby animal ID was known by the investigator, but the experimental group of the animal was not revealed until after analyses were performed. Body weight, blood glucose levels, stress–strain, and wall parameters (inner and outer diameters, wall thickness, and arterial lengthening) were analysed using repeated-measures two-way ANOVA with Bonferroni post hoc analysis. Post hoc analysis was only performed when the *F* value was greater than *F* critical value, indicating that there was no variance in homogeneity. HbA1c levels, plasma insulin, AUC, and gene

expression were analysed using a two-way ANOVA, with Fisher's LSD post hoc analysis. Student's t test was used for *AnxA1* gene expression, and a Mann–Whitney test to quantify FPR1 and FPR2 protein immunostaining. $P < .05$ was considered statistically significant. All groups analysed in this study have $n \geq 5$. On occasion outliers were excluded in data analysis and presentation, where indicated on the figure legend. Outlier is predefined when an individual data point is 2 SDs away from the mean.

2.7 | Nomenclature of targets and ligands

Key protein targets and ligands in this article are hyperlinked to corresponding entries in http://www.guidetopharmacology.org, the common portal for data from the IUPHAR/BPS Guide to PHARMACOLOGY (Harding et al., 2018), and are permanently archived in the Concise Guide to PHARMACOLOGY 2019/20 (Alexander et al., 2019).

3 | RESULTS

3.1 | Insulin-resistance mouse model

3.1.1 | Systemic characteristics in vivo

The insulin-resistance model was established using a combination of low-dose STZ and HFD. This combination regimen did not reduce plasma insulin levels but resulted in a gradual rise in blood glucose levels, similar to that observed in insulin-resistant humans (Huynh et al., 2014; Mukherjee, Hossain, Mondal, Paul, & Ghosh, 2013). There were no differences in body weight between any of the experimental groups in the insulin-resistance study, whether sham or insulin-resistant mice (20 weeks of HFD superimposed on low-dose STZ, Figure 1a). Blood glucose levels were significantly elevated in both *AnxA1*^{+/+} and *AnxA1*^{−/−} insulin-resistant mice (Figure 1b). Notably, this level of hyperglycaemia was lower than that observed in insulin-deficient mice. Similarly, both *AnxA1*^{+/+} and *AnxA1*^{−/−} insulin-resistant
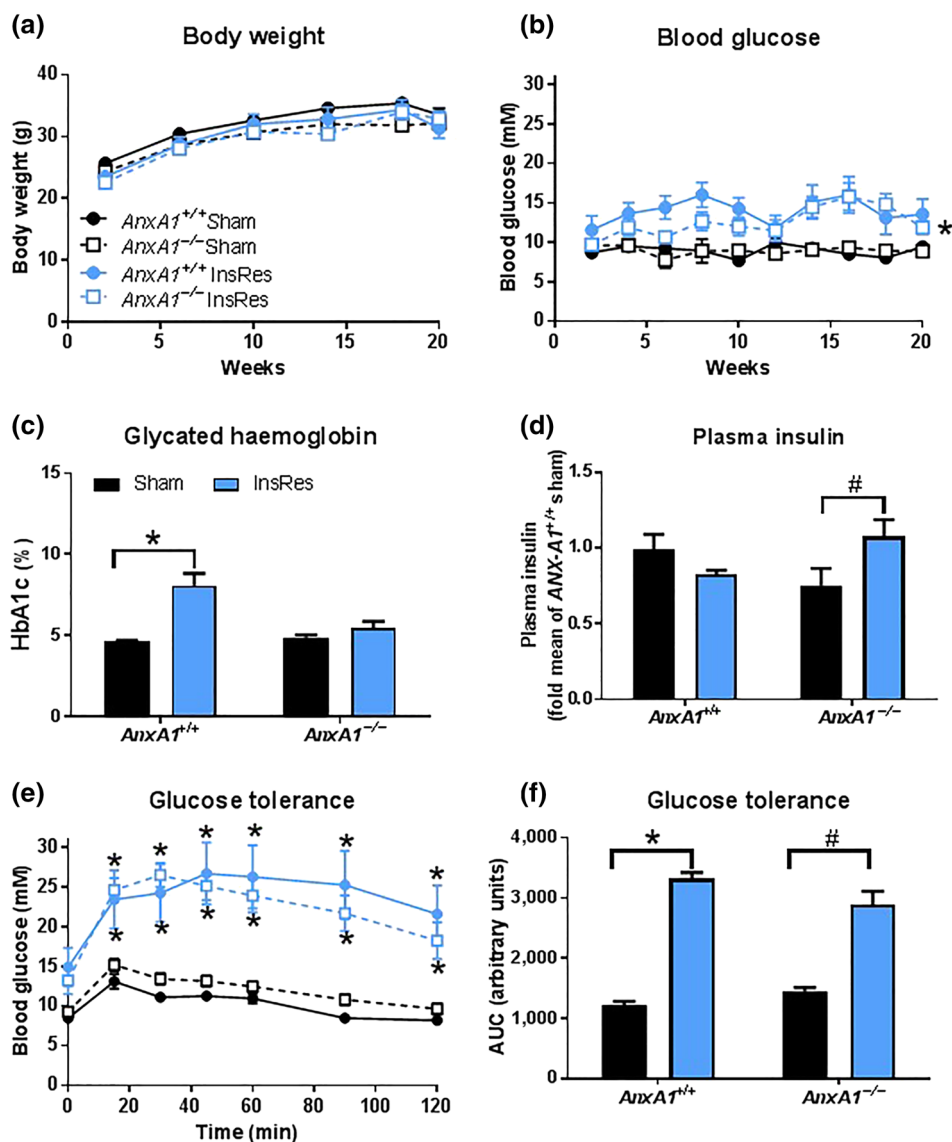

FIGURE 1 Effects of insulin resistance on body weight, blood glucose, and glycated Hb. (a) Body weight (g), (b) blood glucose (mM), (c) Endpoint HbA1c (%), (d) plasma insulin (represented as fold compared to *AnxA1*^{+/+} sham group), and glucose tolerance, both (e) over time and (f) AUC in sham *AnxA1*^{+/+} ($n = 10$), sham *AnxA1*^{−/−} ($n = 7$), insulin-resistant (InsRes) *AnxA1*^{+/+} ($n = 6$), and insulin-resistant *AnxA1*^{−/−} ($n = 14$) male mice. Values are mean ± SEM. *$P < .05$, significantly different from sham *AnxA1*^{+/+}, #$P \leq .05$, significantly different from *AnxA1*^{−/−} sham mice. (a), (b), and (e) were analysed using repeated-measures two-way ANOVA with Bonferroni post hoc analysis. (c), (d), and (f) were analysed using a two-way ANOVA with Fisher's LSD post hoc analysis

mice exhibited significantly increased blood glucose levels during glucose tolerance tests, compared with shams (Figure 1e,f). Interestingly, HbA1c levels were increased significantly in $AnxA1^{+/+}$ insulin-resistant mice, but not in their corresponding $AnxA1^{-/-}$ counterparts. Post hoc analyses revealed that InsRes $AnxA1^{+/+}$ mice exhibited significantly increased blood glucose levels from 8 weeks after the induction of diabetes, whereas InsRes $AnxA1^{-/-}$ mice only exhibited increased plasma blood glucose levels from 16 weeks after the induction of diabetes. This could explain why the HbA1c levels were not significantly elevated in the $AnxA1^{-/-}$ group, because fasting blood glucose levels were only raised in the final 4 weeks (much less than the lifespan of a red blood cell [3 months]).

This suggests that the impairment in glycaemic control was less severe in $AnxA1^{-/-}$ mice subjected to insulin resistance (Figure 1c). In addition, plasma insulin levels only tended to be increased in $AnxA1^{-/-}$ insulin-resistant mice (Figure 1d). Collectively, these data confirm that the combination of low-dose STZ and HFD combination induced insulin resistance (elevated blood glucose levels, without affecting circulating insulin levels). BP and heart rate were measured in anaesthetised mice in vivo at study endpoint. Neither insulin resistance nor AnxA1 deficiency affected systolic or diastolic BP (Table 1). However, heart rate was significantly increased in $AnxA1^{-/-}$ insulin-resistant mice compared with $AnxA1^{-/-}$ shams (Table 1).

3.1.2 | Passive mechanical wall properties of mesenteric vasculature ex vivo

Mesenteric artery passive inner diameter, outer diameter, and wall cross-sectional area were significantly increased (with pressurisation) in $AnxA1^{+/+}$ insulin-resistant mice compared with all three other experimental groups (Figure 2a,b,d). No differences in wall thickness were observed between groups in the insulin-resistance study (Figure 2c). These findings are indicative of hypertrophic outward remodelling (increased inner diameter and wall cross-sectional area) in $AnxA1^{+/+}$ insulin-deficient mice, but AnxA1 deficiency appeared to impede this remodelling. Analysis of the stress–strain relationship indicated that there was no effect of either insulin resistance or AnxA1 deficiency on mesenteric artery circumferential stiffness

(Figure 3a). Passive volume compliance was also not affected by insulin resistance in either $AnxA1^{+/+}$ or $AnxA1^{-/-}$ mice. However, $AnxA1^{-/-}$ mice exhibited reduced volume compliance compared with $AnxA1^{+/+}$ mice. Post hoc analyses revealed that this was only significant at 40 mmHg in sham animals, and in mid-range pressures (40–60 mmHg) in insulin-resistant mice (Figure 3b,c). Hence, our data suggest that AnxA1 deficiency alone reduced volume compliance in mesenteric artery and that this was further exacerbated in mesenteric arteries from insulin-resistant mice. Mesenteric arteries from non-diabetic $AnxA1^{+/+}$ mice exhibited a significantly greater capacity to lengthen with pressurisation compared with all three other experimental groups studied (Figure 3d). This indicates that insulin resistance and AnxA1 deficiency decrease the ability of the mesenteric artery to lengthen with pressurisation.

3.2 | Insulin-deficient mouse model

3.2.1 | Systemic characteristics in vivo

In contrast to the results from mice with insulin resistance, high-dose STZ-induced insulin deficiency significantly decreased body weight gain, in both $AnxA1^{+/+}$ and $AnxA1^{-/-}$ mice (Figure 4a). Furthermore, this trend for decreased body weight gain was more apparent in $AnxA1^{-/-}$ insulin-deficient mice compared with $AnxA1^{+/+}$ insulin-deficient mice. As expected, insulin deficiency significantly increased blood glucose and glycated Hb (HbA1c) levels, in both $AnxA1^{+/+}$ and $AnxA1^{-/-}$ mice (Figure 4b,c). Plasma insulin levels were lower in $AnxA1^{+/+}$ insulin-deficient mice (Figure 4d), when compared to sham, confirming insulin deficiency. AnxA1 deficiency had no effect on blood glucose levels in non-diabetic sham mice, although plasma insulin levels were significantly reduced in $AnxA1^{-/-}$ sham mice, comparable to those in $AnxA1^{-/-}$ insulin-deficient mice (Figure 4d). BP and heart rate were measured in anaesthetised mice in vivo at study endpoint. Systolic BP was significantly lower in insulin-deficient mice compared to sham mice, regardless of genotype (Table 1). Diastolic BP and heart rate were not significantly different across all four experimental groups in the insulin deficiency study (Table 1).

TABLE 1 BP and heart rate in insulin-resistant and insulin-deficient $AnxA1^{+/+}$ and $AnxA1^{-/-}$ male mice

| | Insulin-resistant study | | | | Insulin-deficient study | | | |
| | Sham | | Insulin resistant | | Sham | | Insulin deficient | |
	$AnxA1^{+/+}$	$AnxA1^{-/-}$	$AnxA1^{+/+}$	$AnxA1^{-/-}$	$AnxA1^{+/+}$	$AnxA1^{-/-}$	$AnxA1^{+/+}$	$AnxA1^{-/-}$
SBP (mmHg)	97 ± 2 (10)	107 ± 6 (6)	107 ± 6 (5)	123 ± 5 (13)	117 ± 6 (8)	116 ± 5 (7)	93 ± 3* (5)	95 ± 5* (5)
DBP (mmHg)	66 ± 2 (10)	70 ± 4 (6)	68 ± 7 (5)	81 ± 3 (13)	74 ± 4 (8)	79 ± 4 (7)	63 ± 2 (5)	63 ± 7 (5)
HR (BPM)	409 ± 4 (10)	401 ± 10 (6)	404 ± 13 (5)	446 ± 14[#] (13)	401 ± 8 (8)	404 ± 13 (7)	399 ± 20 (5)	412 ± 19 (5)

Note. Values are mean ± SEM with *n* indicated in parentheses. Data were analysed using two-way ANOVA with Fisher's LSD post hoc analysis.
Abbreviations: SBP, systolic BP; DBP, diastolic BP; HR, heart rate.
[*]$P < .05$, significantly different from sham $AnxA1^{+/+}$.
[#]$P < .05$, significantly different from sham $AnxA1^{+/+}$.

FIGURE 2 Effects of insulin resistance on passive mesenteric artery wall parameters. (a) Inner and (b) outer diameters, (c) wall thickness, and (d) wall CSA over the pressurisation range (5–120 mmHg) in sham $AnxA1^{+/+}$ (n = 10), sham $AnxA1^{−/−}$ (n = 6), insulin-resistant (InsRes) $AnxA1^{+/+}$ (n = 6), and insulin-resistant $AnxA1^{−/−}$ (n = 15) male mice. Values are mean ± SEM. *$P < .05$, significantly different from $AnxA1^{+/+}$ sham mice. Data were analysed using repeated-measures two-way ANOVA with Bonferroni post hoc analysis
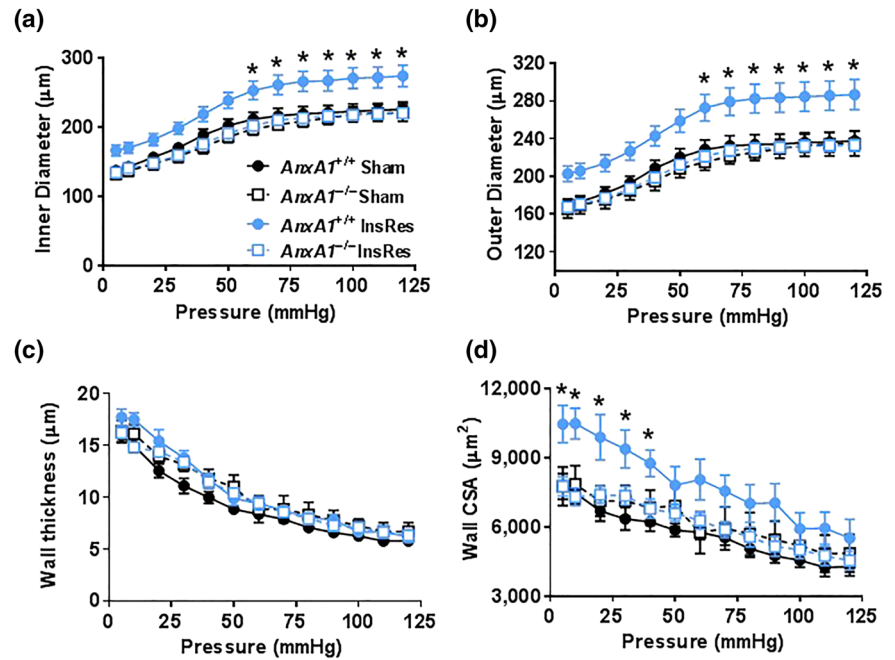
3.2.2 | Passive mechanical wall properties of mesenteric vasculature ex vivo

Mesenteric artery passive inner and outer diameters were significantly increased (with pressurisation) in both $AnxA1^{+/+}$ and $AnxA1^{−/−}$ insulin-deficient mice throughout the whole pressurisation range (Figure 5a,b). Conversely, there were no differences in wall thickness between all experimental groups in the insulin deficiency study (Figure 5c). Although vessel wall cross-sectional area was increased (with pressurisation) in insulin-deficient mice, this was only significant in $AnxA1^{+/+}$ mice (Figure 5d). Together, these findings suggest hypertrophic outward remodelling in $AnxA1^{+/+}$, and eutrophic remodelling (increased inner diameter but no change in cross-sectional area) in

$AnxA1^{−/−}$ mice, in the context of insulin deficiency. There were no significant differences in the stress–strain relationship of the mesenteric arteries between $AnxA1^{−/−}$ and $AnxA1^{+/+}$ sham mice, nor between sham and insulin-deficient $AnxA1^{+/+}$ mice. Conversely, the stress–strain curve was significantly shifted to the right in $AnxA1^{−/−}$ insulin-deficient mice (compared with all three other experimental groups), indicating reduced circumferential stiffness (Figure 6a). Surprisingly, insulin deficiency significantly increased volume compliance in mesenteric arteries, independent of genotype (both $AnxA1^{+/+}$ and $AnxA1^{−/−}$ mice), indicating a possible compensatory reduction in longitudinal stiffness (Figure 6b,c). Although there was no effect of AnxA1 deficiency on volume compliance, there were differences between genotypes in arterial lengthening. Specifically, percentage

FIGURE 3 Effects of insulin resistance on passive mechanical wall properties. (a) Stress–strain relationships; (b) volume compliance (over the pressurisation range) and (c) AUC for volume compliance; (d) % change in length (over the pressurisation range) in sham $AnxA1^{+/+}$ (n = 8), sham $AnxA1^{−/−}$ (n = 5), insulin-resistant (InsRes) $AnxA1^{+/+}$ (n = 7), and insulin-resistant $AnxA1^{−/−}$ (n = 14) male mice. Values are mean ± SEM. *$P < .05$, significantly different from sham $AnxA1^{+/+}$, §$P < .05$, significantly different from $AnxA1^{+/+}$ insulin-resistant mice. (a), (b), and (d) were analysed using repeated-measures two-way ANOVA with Bonferroni post hoc analysis, whereas (c) were analysed using two-way ANOVA with Fisher's LSD post hoc analysis. $P < .05$ was considered statistically significant
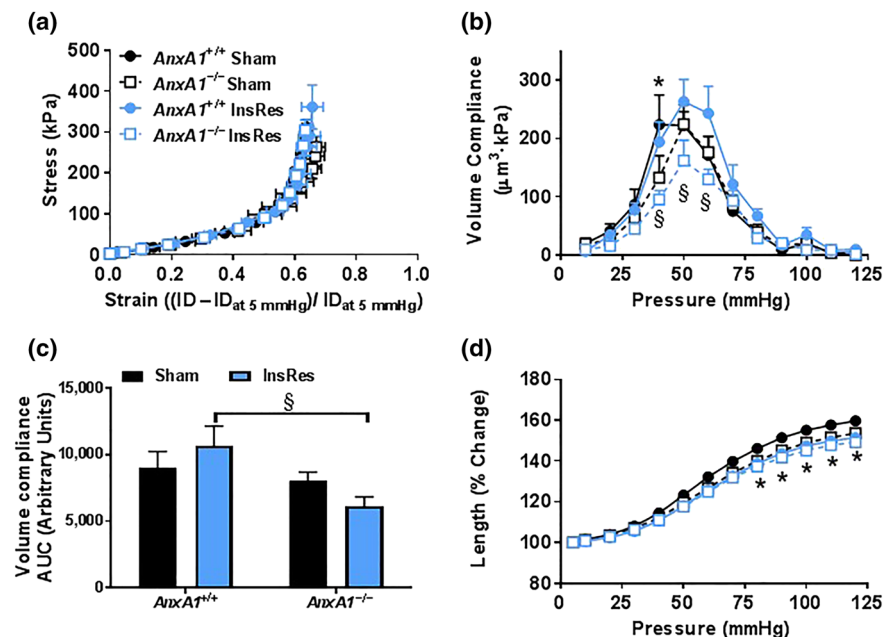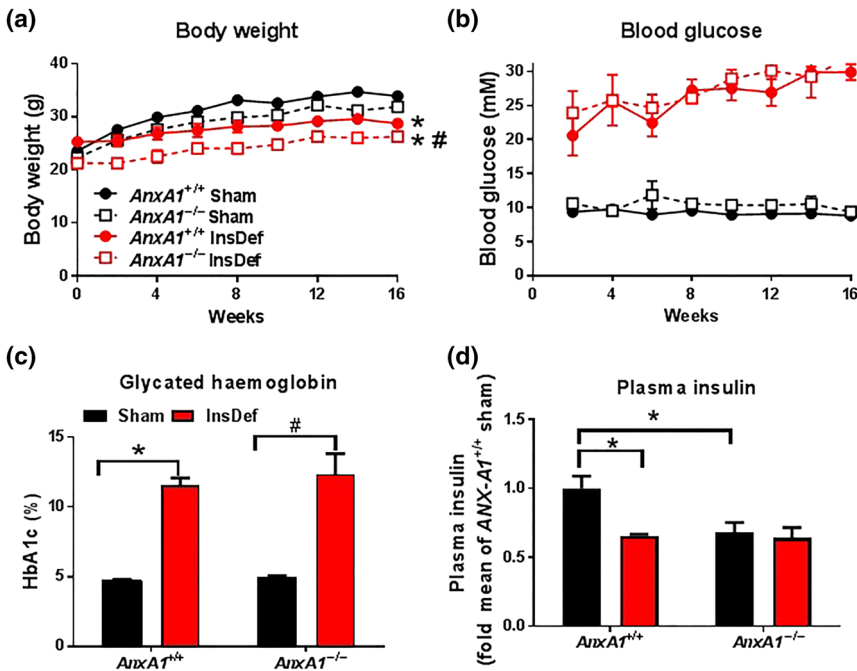
FIGURE 4 Effects of insulin deficiency on body weight, blood glucose, and glycated Hb. (a) Body weight (g) and (b) blood glucose (mM) measures during treatment in sham (circles) and insulin-deficient (InsDef;) $AnxA1^{+/+}$ and $AnxA1^{-/-}$ male mice. (c) Endpoint glycated haemoglobin (HbA1c, %) and (d) plasma insulin levels were also determined (represented as fold compared to $AnxA1^{+/+}$ sham group). Sham $AnxA1^{+/+}$ ($n = 10$), sham $AnxA1^{-/-}$ ($n = 7$), insulin-deficient $AnxA1^{+/+}$ ($n = 6$), and insulin-deficient $AnxA1^{-/-}$ ($n = 12$) male mice. Values are mean ± SEM. *$P < .05$, significantly different from sham $AnxA1^{+/+}$, #$P < .05$, significantly different from $AnxA1^{-/-}$ sham mice. (a) and (b) were analysed using repeated-measures two-way ANOVA with Bonferroni post hoc analysis. (c) and (d) were analysed using a two-way ANOVA with Fisher's LSD post hoc analysis

change in length with pressurisation was significantly increased in $AnxA1^{+/+}$ insulin-deficient mice compared with $AnxA1^{+/+}$ shams. Conversely, no differences in arterial lengthening were observed between sham and insulin-deficient $AnxA1^{-/-}$ mice (Figure 6d).

3.2.3 | The role of the AnxA1 pathway in insulin resistance and insulin deficiency

To further investigate the vascular role of AnxA1 in the settings of insulin resistance and insulin deficiency, we measured the expression of $mAnxA1$, $mFpr1$, and $mFpr2$ genes. Interestingly, we found that

$mAnxA1$ expression was significantly up-regulated in both insulin-resistant and insulin-deficient $AnxA1^{+/+}$ mice (Figure 7a). $mFpr1$ expression was up-regulated in both insulin-deficient and insulin-resistant mice, whereas $mFpr2$ was only significantly increased in insulin-deficient mice, regardless of genotype (Figure 7b,c), as revealed by two-way ANOVA. Post hoc analysis revealed greater than fivefold up-regulation of mFpr1 in $AnxA1^{-/-}$ mice, significantly higher than the levels in their wild-type counterparts. We also measured expression of a key pro-inflammatory cytokine gene $mMcp-1$, coding for the chemokine CCL2. Consistent with the increased AnxA1/FPR axis, a significant up-regulation of expression of $mMCP-1$ was observed in insulin-resistant and insulin-deficient mice. Interestingly,
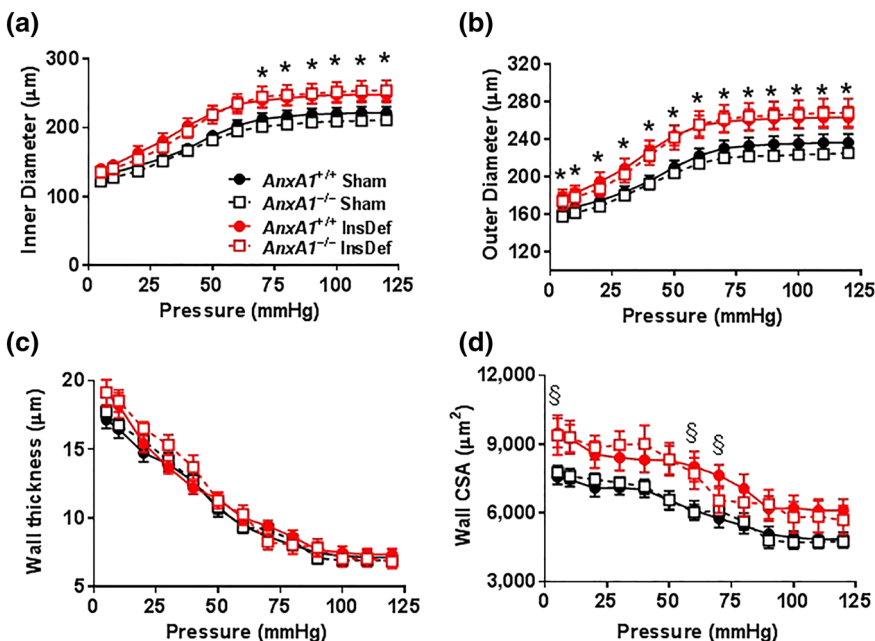

FIGURE 5 Effects of insulin deficiency on passive mesenteric artery wall parameters. (a) Inner and (b) outer diameters, (c) wall thickness, and (d) wall cross-sectional area (CSA) over the pressurisation range (5–120 mmHg) in sham $AnxA1^{+/+}$ ($n = 14$), sham $AnxA1^{-/-}$ ($n = 10$), insulin-deficient (InsDef) $AnxA1^{+/+}$ ($n = 10$), and insulin-deficient $AnxA1^{-/-}$ ($n = 8$) male mice. Values are mean ± SEM. *$P < .05$, significantly different from sham $AnxA1^{+/+}$, §$P < .05$, significantly different from $AnxA1^{+/+}$ insulin-deficient mice. Data were analysed using repeated-measures two-way ANOVA with Bonferroni post hoc analysis

FIGURE 6 Effects of insulin deficiency on passive mechanical properties of vascular walls. (a) Stress–strain relationship; (b) volume compliance (over the pressurisation range) and (c) AUC for volume compliance; and (d) % change in length (over the pressurisation range) in sham $AnxA1^{+/+}$ ($n = 14$), sham $AnxA1^{-/-}$ ($n = 8$), insulin-deficient (InsDef) $AnxA1^{+/+}$ ($n = 13$), and insulin-deficient $AnxA1^{-/-}$ ($n = 8$) male mice. Values are mean ± SEM. $^{\#}P < .05$, significantly different from all other groups; $^{*}P < .05$, significantly different from sham $AnxA1^{+/+}$, $^{\#}P < .05$, significantly different from significantly different from $AnxA1^{-/-}$ sham mice, $^{\S}P < .05$, significantly different from $AnxA1^{+/+}$ insulin-deficient mice. (a), (b), and (d) were analysed using repeated-measures two-way ANOVA with Bonferroni post hoc analysis, whereas (c) were analysed using two-way ANOVA with Fisher's LSD post hoc analysis
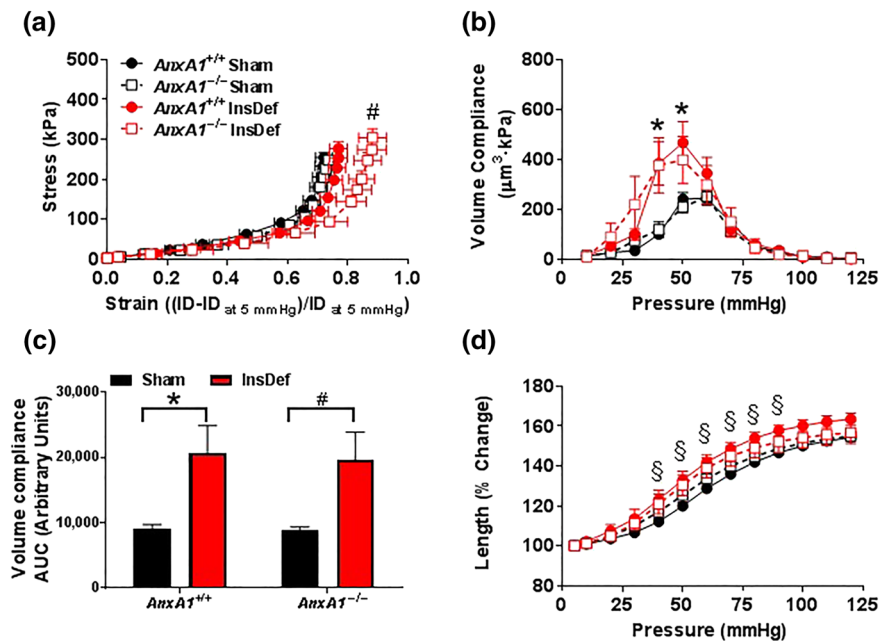
deficiency in $AnxA1$ leads to increased $mFpr1$ and $mMcp-1$ in insulin-resistant mice. An outlier in insulin-deficient $AnxA1^{-/-}$ mice was identified and thus excluded for further analysis. We performed immunohistochemistry to localise FPR1 and FPR2 in the mesenteric artery. Both FPR1 and FPR2 were present in the vascular smooth muscle cells, and limited in endothelial cells, in the representative images obtained in the sham wild-type mice.

Staining for FPR2 tended to be stronger than that for FPR1 ($P=0.06$, Mann-Whitney test), suggesting that there may be a more prominent role for FPR2 in the mesenteric artery than FPR1 (Fig 7D). Control serum revealed no staining.

4 | DISCUSSION AND CONCLUSIONS

The main finding of this study is the contribution of endogenous AnxA1 to mesenteric artery structure, with the extent of the effects being dependent on the phenotype of diabetes. Our study is the first to localise receptors for AnxA1 (FPR1 and FPR2) in the vascular smooth muscle of mesenteric arteries. Intriguingly, our findings suggest that deficiency of $AnxA1$ exacerbated the development of key characteristics of vascular stiffness (reduced artery compliance) only in the setting of insulin resistance, but not insulin deficiency. Thus, our study demonstrates for the first time that $AnxA1$ deficiency is detrimental to the vasculature in the setting of insulin resistance.

The insulin-resistant and insulin-deficient animal models of diabetes used in this study resulted in distinct differences between vascular phenotypes (as summarised in Figure 8 and Table 2). Specifically, insulin-deficient mice exhibited hyperglycaemia throughout the whole treatment period, with decreased body weight gain and reduced circulating insulin levels by study endpoint. Conversely, insulin-resistant

mice exhibited a delayed, and much milder level of, hyperglycaemia, which was even milder in the $AnxA1^{-/-}$ mice. This is surprising considering that $AnxA1$ deficiency exacerbated pathological remodelling in the context of insulin resistance, despite this delayed, milder hyperglycaemia. Although there was a concomitant impairment in glucose tolerance, there were no differences in body weight or plasma insulin levels in insulin-resistant mice. Thus, our study represents two distinct disease settings, severe hyperglycaemia with insulin deficiency in both $AnxA1^{+/+}$ and $AnxA1^{-/-}$ mice (analogous to T1D), and mild hyperglycaemia with insulin resistance in both genotypes. These differences may contribute to the differential vascular phenotypes observed in the two models.

The mRNA for FPR2 is detectable in endothelial cells (HUVECs) and sections of lung tissue (Koczulla et al., 2003). We have however now provided immunostaining data to show that the FPRs are present in the mesenteric artery in $AnxA1^{+/+}$ mice. Importantly, this is the first report to demonstrate AnxA1 receptors (FPR1 and FPR2) in the mesenteric vasculature. Our data suggest that FPR2 is more prevalent than FPR1 in this vascular bed and provides some of the first evidence that AnxA1 could be acting directly on the vascular smooth muscle cells to elicit vasoprotective effects in the mesenteric artery. Our study is also the first to show that $AnxA1$ deficiency may exacerbate vascular remodelling, specifically in the context of diabetes, an effect that is dependent on the nature of the diabetic phenotype: insulin deficiency or insulin resistance. Despite the differences observed between the two models of diabetes, gene expression of $AnxA1$, its receptors $Fprs$, and the key inflammatory cytokine $Mcp-1$ were up-regulated in the mesenteric vasculature in both insulin deficiency and insulin resistance. Interestingly, deficiency of $AnxA1$ is sufficient to create a pro-inflammatory environment in the microvasculature. However, given the limited availability of remaining tissue, we are unable
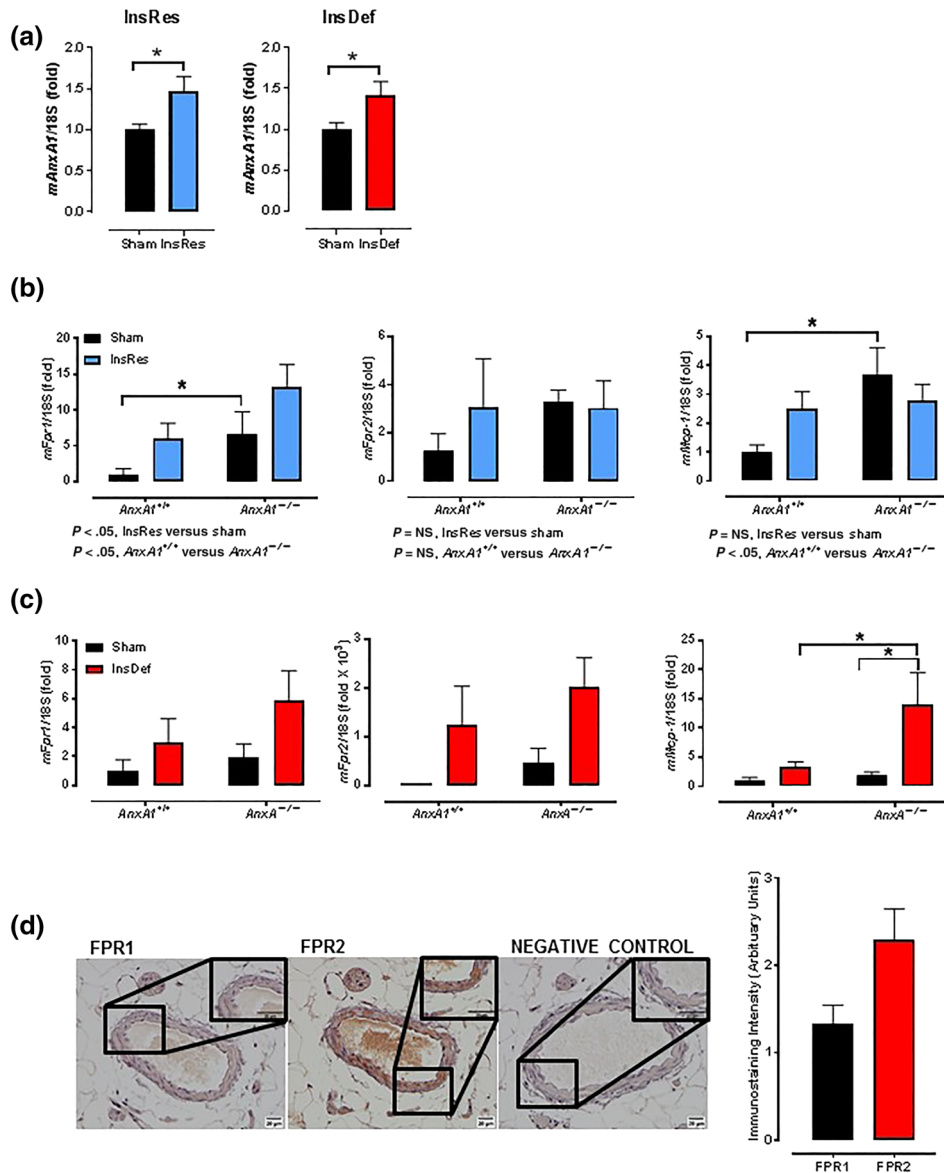
FIGURE 7 Expression and localisation of the AnxA1/FPR system in insulin-resistant and insulin-deficient mice. *mAnxA1* (a), *mFpr1*, *mFpr2*, and *mMCP-1* mRNA expression in mesenteric arteries of insulin-resistant (InsRes, b) and insulin-deficient (InsDef, c) male mice. Sham *AnxA1*^{+/+} and *AnxA1*^{−/−} (n = 6); insulin-deficient *AnxA1*^{+/+} and *AnxA1*^{−/−} (n = 6); insulin-resistant *AnxA1*^{+/+} and *AnxA1*^{−/−} (n = 6) male mice. Localisation (representative image) and quantification of FPRs in mesenteric arteries (d, n = 5–7). Insert highlights a region within the blood vessel (magnification ×100). VSMCs, vascular smooth muscle cells; EC, endothelial cell; *mFpr1*, formyl peptide receptor 1 gene; *mFpr2*, formyl peptide receptor 2 gene; FPR1, formyl peptide receptor 1 protein; FPR2, formyl peptide receptor 2 protein. Values are mean ± SEM. An outlier in insulin-deficient *AnxA1*^{−/−} mice is predefined when an individual data point is 2 SDs away from the mean. *$P < 0.05$, significantly different as indicated. (a) was analysed using unpaired Student's *t* test, (b) and (c) were analysed using repeated-measures two-way ANOVA with Bonferroni post hoc analysis

to provide further information at the protein level. Further studies will be needed to elucidate the detailed mechanism(s) that contributes to vascular remodelling in diabetic mice deficient in *AnxA1*.

The effects of AnxA1 on vascular remodelling have been studied in other cardiovascular pathologies (e.g., atherosclerosis), but not in the specific context of diabetes. Previous reports demonstrated that the response of *ApoE*^{−/−} mice fed a high-cholesterol diet subjected to wire injury, particularly at the level of neointima thickness, is

aggravated by the absence of endogenous AnxA1 (de Jong et al., 2017). Administration of exogenous AnxA1 attenuates the progression of established atherosclerotic plaques in mice deficient in LDL receptor, fed with a western-type diet (LDLR^{−/−}; Kusters et al., 2015), but the effect of AnxA1 on vascular remodelling (away from regions of plaque) was not determined. Neither of these previous studies examined the effects of AnxA1 (endogenous or exogenous) on arterial passive mechanics, volume compliance, or

FIGURE 8 Summary of the role of endogenous Annexin-A1 in the context of insulin resistance, as distinct from insulin deficiency. *AnxA1* deficiency decreases vessel compliance in insulin-resistant mice. Conversely, AnxA1 deficiency has no effects on vessel compliance in normal and insulin-deficient mice. Schema created using a modification to an image provided by Servier Medical Art by Servier (http://www.servier.com/ Powerpoint-image-bank), licensed using a Creative Commons Attributes 3.0 Unported Licence (http:// creativecommons.com/licence/by/3.0)
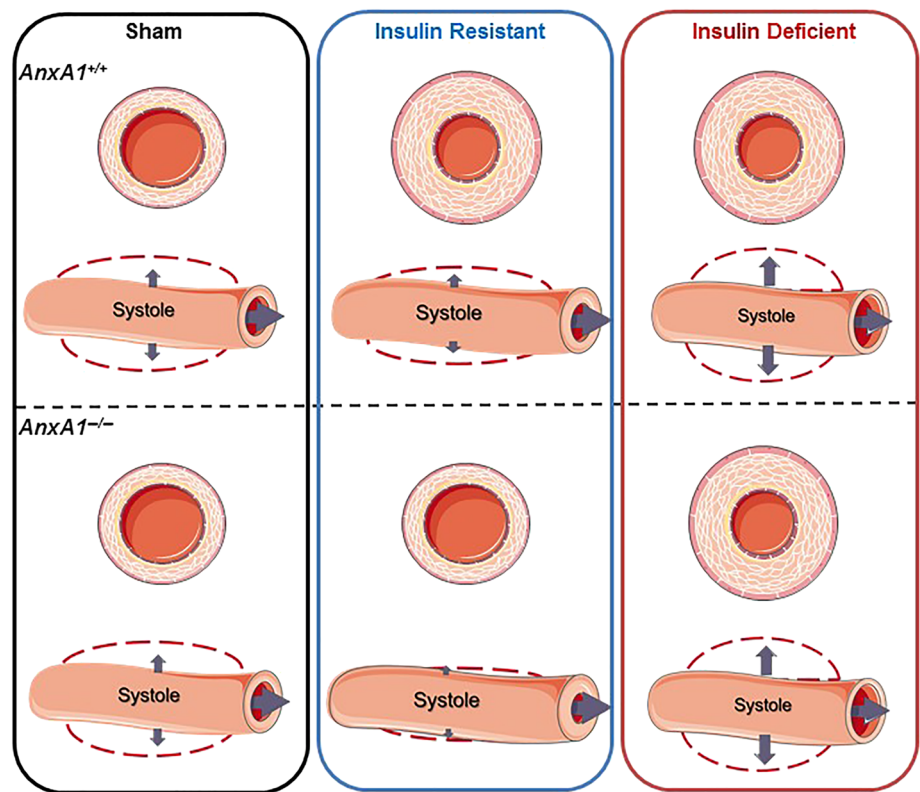

TABLE 2 Summary of the phenotypes of insulin-resistant and insulin-deficient $AnxA1^{+/+}$ and $AnxA1^{-/-}$ male mice compared with $AnxA1^{+/+}$ sham controls

	Insulin-resistant study			Insulin-deficient study		
	$AnxA1^{-/-}$ sham	$AnxA1^{+/+}$ InsRes	$AnxA1^{-/-}$ InsRes	$AnxA1^{-/-}$ sham	$AnxA1^{+/+}$ InsDef	$AnxA1^{-/-}$ InsDef
Body weight	↔	↔	↔	↔	↓	↓↓
Blood glucose	↔	↑	↑	↔	↑↑	↑↑
GTT	↔	↑	↑	ND	ND	ND
HbA1c	↔	↑	↔	↔	↑	↑
Plasma insulin	↔	↔	↔	↓	↓	↓
Systolic BP	↔	↔	↔	↔	↓	↓
Heart rate	↔	↔	↑	↔	↔	↔
Vascular Remodelling	None	Outward (hypertrophic)	None	None	Outward (hypertrophic)	Outward (eutrophic)
Circumferential stiffness	↔	↔	↔	↔	↔	↓
Volume compliance	↓	↔	↓	↔	↑	↑
Arterial lengthening	↓	↓	↓	↔	↑	↔

Abbreviations: GTT, glucose tolerance test; HbA1c, glycated Hb; ND, not determined.

arterial stiffness, nor was the effect on resistance (as opposed to conduit) arteries examined.

In the mesenteric arteries of $AnxA1^{+/+}$ mice, insulin-deficiency was associated with reduced axial stiffness, whereas insulin resistance had no effect on stiffness or compliance. These observations are consistent with our recent study in STZ-induced T1D rats, in which both moderate (20-mM blood glucose) and severe hyperglycaemia (30-mM

blood glucose) increased axial, but not circumferential, stiffness in mesenteric arteries (Kahlberg et al., 2016). However, the effects of T1D on vascular stiffness remain controversial, as arterial stiffness was observed in rat cremaster arterioles (Hill et al., 1994) and in femoral artery, but had no effect in mesenteric arteries (Wigg et al., 2004). Different phenotypes of diabetes exhibit varying effects in different vascular beds; discrepancies in the literature may also reflect the use

of different animal strains (Wistar or. Sprague Dawley) or species (rats or mice). Our study is consistent with published studies in that body weight gain was decreased in insulin-deficient rats (Kahlberg et al., 2016). Interestingly, the STZ/HFD-induced insulin-resistant mice did not exhibit decreased body weight gain. It is possible that the high-fat diet may compensate for potential decreased weight gain as a result of the administration of low dose of STZ. High dose of STZ administration has been associated with decreased weight gain (Kahlberg et al., 2016).

One possible explanation that accounts for the difference in vascular phenotype observed between the two mouse models is body weight, which is an important contributing factor to haemodynamic (and in turn net vascular remodelling and passive mechanics; Doevendans, Daemen, de Muinck, & Smits, 1998). In the present investigation, diabetes was induced from 6 weeks of age, when mice were still in a growth phase, with decreased body weight gain in the insulin-deficient mice. Substantial (~20%) vascular development also occurs in the mesenteric vasculature during this growth phase (Unthank et al., 1987), both circumferentially and axially. Thus, the effect of this altered weight gain in the insulin-deficient mice during this growth phase may have contributed to vascular remodelling observed in these mice. InsDef mice exhibited retarded body weight gain, consistent with our previous report in this model (Ng et al., 2017). Interestingly, $AnxA1^{-/-}$ mice exhibited lower body weight at study commencement, compared to $AnxA1^{+/+}$ mice. We suggest that the difference between the InsDef $AnxA1^{+/+}$ and $AnxA1^{-/-}$ mice is predominantly due to the lower starting bodyweight, rather than deficiency in insulin. Similarly, HFD-induced bodyweight gain also affects vascular remodelling, by promoting vascular stiffness in the aorta and mesenteric arteries (Foote et al., 2016; Santana et al., 2014), further supporting the influence of bodyweight on vascular remodelling and passive mechanics in this study. Hence, the decreased body weight gain in insulin-deficient mice may reflect an adaptive, compensatory mechanism rather than a pathological response. Given that the blood supply to the mesentery increases in diabetes (Hill et al., 1989) and that the insulin-deficient mice studied here exhibited a lower BP, compared with control mice (at least under anaesthesia), this observation is consistent with reduced mesenteric artery axial stiffness in these mice. Despite increased mesenteric artery stiffness in insulin-resistant mice, deficiency in $AnxA1$ did not affect BP measurements (under anaesthesia). This could be due to compensatory effects on vascular function or haemodynamics and further studies are required to elucidate these mechanisms. The effects of AnxA1 deficiency on BP in conscious animals remains to be investigated.

A number of previous studies have reported that mesenteric arteries from both insulin-deficient (Crijns et al., 1999; Kahlberg et al., 2016; Pourageaud et al., 1997) and insulin-resistant rodents (Souza-Smith et al., 2011) undergo hypertrophic outward remodelling. We also observed this phenomenon in $AnxA1^{+/+}$ mice from both insulin-resistant and insulin-deficient models of diabetes. In contrast, $AnxA1^{-/-}$ mice exhibited different types of vascular remodelling, dependent on the disease phenotype. Insulin deficiency induced eutrophic outward remodelling in $AnxA1^{-/-}$ mice, accompanied by reduced arterial stiffness, suggesting that AnxA1 deficiency may not be detrimental in the context of T1D. This suggests that there may be compensatory mechanisms in the vasculature of $AnxA1^{-/-}$ mice to enable them to better adapt to the challenge of insulin deficiency. Insulin resistance had no effects on artery wall parameters in $AnxA1^{-/-}$ mice but was associated with a reduction in volume compliance. This indicates that in the absence of AnxA1, volume compliance is compromised in the setting of insulin resistance. Furthermore, $AnxA1^{-/-}$ InsRes mice and $AnxA1^{+/+}$ sham mice were significantly different at low intraluminal pressure (40 mmHg), suggesting that AnxA1 might play an important physiological role in regulating mesenteric arterial stiffness. Reduction in arterial compliance may precede (and exacerbate) the onset of diseases such as hypertension and atherosclerosis and may help to identify individuals at risk before the onset of symptom (Glasser et al., 1997). Another potential explanation for why $AnxA1$ deficiency exerted different effects in the two different models of diabetes is that AnxA1 is endogenously expressed in the islets of the pancreas, where it co-localises with insulin secretory granules, and may influence glucose-stimulated insulin secretion in an autocrine or paracrine manner (Ohnishi et al., 1995). In addition, AnxA1 is known to modulate islet function to enhance glucose-stimulated insulin secretion (Rackham et al., 2016). In InsDef mice, secretion is reduced, whereas in the Insulin resistance (InsRes) mice, secretion is maintained (and probably eventually increases). It is thus possible that Anx-A1 deficiency leads to dysregulation of insulin secretion, resulting in elevated insulin plasma level in insulin-resistant mice. This may explain why $AnxA1$ deficiency exerts different effects in the two different models of diabetes.

Importantly, $AnxA1^{-/-}$ insulin-resistant mice also exhibited increased heart rate, which could potentially reflect increased activation of the sympathetic nervous system (as occurs in human diabetics), which may also contribute to the observed reduction in volume compliance (Bellien et al., 2010; Sasson et al., 2012). Although such a possibility was beyond the scope of the present study, previous reports in T2D mice demonstrate that haemodynamic changes precede mesenteric artery remodelling (Raskin & Mohan, 2010). Nevertheless, our study suggests that $AnxA1$ deficiency is detrimental to the mesenteric vasculature in insulin-resistant mice. Thus, endogenous AnxA1 may play a protective role in the settings of insulin resistance, supporting the potential use of AnxA1 pharmacotherapy to alleviate microvascular complications in T2D.

The results presented here indicate that insulin deficiency induces outward remodelling and reduced axial stiffness, in both $AnxA1^{+/+}$ and $AnxA1^{-/-}$ mice. In contrast, insulin resistance has differential effects depending on the genotype. $AnxA1^{+/+}$ mice with insulin resistance exhibit outward remodelling but not vascular stiffness. Conversely, insulin-resistant $AnxA1^{-/-}$ mice exhibit stiffer mesenteric arteries, with no difference in wall parameters. Our study is the first to compare systemic resistance artery stiffness in models of insulin resistance and insulin deficiency. Furthermore, we demonstrated for the first time that endogenous AnxA1 exaggerates vascular stiffness specifically in insulin-resistant mice, consistent with the anti-inflammatory properties of AnxA1. The limited availability of

mesenteric artery tissue however prevented us from assessing if this increased vascular stiffness was associated with increased intima-media thickness or collagen deposition. Further studies are now warranted to identify the full effects of endogenous AnxA1 in the vasculature and the associated molecular mechanisms by which it acts, particularly in the context of insulin resistance. Whether the increased mesenteric vascular stiffness evident in $AnxA1^{-/-}$ insulin-resistant mice could be rescued by exogenous AnxA1 or its mimetic remains to be determined. AnxA1-based strategies may represent a novel therapy to reduce vascular damage in patients suffering diabetes.

In conclusion, our data reveal that endogenous AnxA1 has diabetes-specific effects on mesenteric artery passive mechanics (summarised in Figure 8). This observation is the first study to examine the contribution of endogenous AnxA1 to passive mechanical properties of the vascular wall in the context of insulin resistance in vivo. Our data reveal compelling new insights for the development of AnxA1-based strategies for treating vascular stiffness in patients, associated with insulin resistance.

AUTHOR CONTRIBUTIONS

M.J., N.K., C.H.L., C.X.Q., and R.H.R. designed the research; M.J., N.K., C.H.L., H.H.N., S.R., M.D., M.L., S.F., and C.X.Q. collected and analysed the data; M.J., C.H.L., H.H.N., L.J.P., C.X.Q., and R.H.R. interpreted the data. M.J., N.K., J.W., L.J.P., C.X.Q., and R.H.R. drafted the manuscript. All authors approved the final version of the manuscript.

CONFLICT OF INTEREST

The authors declare no conflicts of interest.

DECLARATION OF TRANSPARENCY AND SCIENTIFIC RIGOUR

This Declaration acknowledges that this paper adheres to the principles for transparent reporting and scientific rigour of preclinical research as stated in the BJP guidelines for Design & Analysis, Immunoblotting and Immunochemistry, and Animal Experimentation, and as recommended by funding agencies, publishers and other organisations engaged with supporting research.

ORCID

Chen Huei Leo [iD] https://orcid.org/0000-0003-1424-9694
Hooi Hooi Ng [iD] https://orcid.org/0000-0002-2370-0849
Cheng Xue Qin [iD] https://orcid.org/0000-0003-2169-2686

REFERENCES

Alexander, S. P. H., Christopoulos, A., Davenport, A. P., Kelly, E., Mathie, A., Peters, J. A., ... Collaborators, C. G. T. P. (2019). THE CONCISE GUIDE TO PHARMACOLOGY 2019/20: G protein-coupled receptors. *British Journal of Pharmacology*, *176*, S21–S141. https://doi.org/10.1111/bph.14748

Alexander, S. P. H., Roberts, R. E., Broughton, B. R. S., Sobey, C. G., George, C. H., Stanford, S. C., ... Ahluwalia, A. (2018). Goals and practicalities of immunoblotting and immunohistochemistry: A guide for submission to the British Journal of Pharmacology. *British Journal of Pharmacology*, *175*, 407–411. https://doi.org/10.1111/bph.14112

Bellien, J., Favre, J., Iacob, M., Gao, J., Thuillez, C., Richard, V., & Joannidès, R. (2010). Arterial stiffness is regulated by nitric oxide and endothelium-derived hyperpolarizing factor during changes in blood flow in humans. *Hypertension*, *55*, 674–680. https://doi.org/10.1161/HYPERTENSIONAHA.109.142190

Crijns, F. R., Wolffenbuttel, B. H., de Mey, J. G., & Boudier, H. A. S. (1999). Mechanical properties of mesenteric arteries in diabetic rats: Consequences of outward remodeling. *American Journal of Physiology-Heart and Circulatory Physiology*, *276*, H1672–H1677. https://doi.org/10.1152/ajpheart.1999.276.5.H1672

Curtis, M. J., Alexander, S., Cirino, G., Docherty, J. R., George, C. H., Giembycz, M. A., ... Ahluwalia, A. (2018). Experimental design and analysis and their reporting II: Updated and simplified guidance for authors and peer reviewers. *British Journal of Pharmacology*, *175*, 987–993. https://doi.org/10.1111/bph.14153

Damazo, A. S., Sampaio, A. L., Nakata, C. M., Flower, R. J., Perretti, M., & Oliani, S. M. (2011). Endogenous annexin A1 counter-regulates bleomycin-induced lung fibrosis. *BMC Immunology*, *12*, 59–59. https://doi.org/10.1186/1471-2172-12-59

Damazo, A. S., Yona, S., D'Acquisto, F., Flower, R. J., Oliani, S. M., & Perretti, M. (2005). Critical protective role for annexin 1 gene expression in the endotoxemic murine microcirculation. *The American Journal of Pathology*, *166*, 1607–1617. https://doi.org/10.1016/S0002-9440(10)62471-6

de Jong, R. J., Paulin, N., Lemnitzer, P., Viola, J. R., Winter, C., Ferraro, B., ... Soehnlein, O. (2017). Protective aptitude of Annexin A1 in arterial neointima formation in atherosclerosis-prone mice—brief report. *Arteriosclerosis, Thrombosis, and Vascular Biology*, *37*, 312–315. https://doi.org/10.1161/ATVBAHA.116.308744

Devaraj, S., Dasu, M. R., & Jialal, I. (2010). Diabetes is a proinflammatory state: a translational perspective. *Expert Review of Endocrinology and Metabolism*, *5*, 19–28. https://doi.org/10.1586/eem.09.44

Doevendans, P. A., Daemen, M. J., de Muinck, E. D., & Smits, J. F. (1998). Cardiovascular phenotyping in mice. *Cardiovascular Research*, *39*, 34–49. https://doi.org/10.1016/s0008-6363(98)00073-x

Foote, C. A., Castorena-Gonzalez, J. A., Ramirez-Perez, F. I., Jia, G., Hill, M. A., Reyes-Aldasoro, C. C., & Martinez-Lemus, L. A. (2016). Arterial stiffening in western diet-fed mice is associated with increased vascular elastin, transforming growth factor-β, and plasma neuraminidase. *Frontiers in Physiology*, *7*, 285–285.

Gavins, F. N. E., Dalli, J., Flower, R. J., Granger, D. N., & Perretti, M. (2007). Activation of the annexin 1 counter-regulatory circuit affords protection in the mouse brain microcirculation. *The FASEB Journal*, *21*, 1751–1758. https://doi.org/10.1096/fj.06-7842com

Glasser, S. P., Arnett, D. K., McVeigh, G. E., Finkelstein, S. M., Bank AJ, Morgan, D. J., & Cohn, J. N. (1997). Vascular compliance and cardiovascular disease: A risk factor or a marker? *American Journal of*

Hypertension, 10, 1175–1189. https://doi.org/10.1016/s0895-7061 (97)00311-7

Hanley, A. J. G., Festa, A., D'Agostino, R. B. J., Wagenknecht, L. E., Savage, P. J., Tracy, R. P., ... Haffner, S. M. (2004). Metabolic and inflammation variable clusters and prediction of type 2 diabetes: Factor analysis using directly measured insulin sensitivity. *Diabetes*, 53, 1773–1782. https://doi.org/10.2337/diabetes.53.7.1773

Hannon, R., Croxtall, J. D., Getting, S. J., Roviezzo, F., Yona, S., Paul-Clark, M. J., ... Flower, R. J. (2003). Aberrant inflammation and resistance to glucocorticoids in annexin $1^{-/-}$ mouse. *The FASEB Journal*, 17, 253–255. https://doi.org/10.1096/fj.02-0239fje

Harding, S. D., Sharman, J. L., Faccenda, E., Southan, C., Pawson, A. J., Ireland, S., ... NC-IUPHAR (2018). The IUPHAR/BPS Guide to PHARMACOLOGY in 2018: Updates and expansion to encompass the new guide to IMMUNOPHARMACOLOGY. *Nucleic Acids Research*, 46, D1091–D1106. https://doi.org/10.1093/nar/gkx1121

Henry, R. M. A., Kostense, P. J., Spijkerman, A. M. W., Dekker, J. M., Nijpels, G., Heine, R. J., ... Hoorn Study (2003). Arterial stiffness increases with deteriorating glucose tolerance status: The Hoorn Study. *Circulation*, 107, 2089–2095. https://doi.org/10.1161/01.CIR.0000065222.34933.FC

Hill, M. A., & Ege, E. A. (1994). Active and passive mechanical properties of isolated arterioles from STZ-induced diabetic rats: Effect of aminoguanidine treatment. *Diabetes*, 43, 1450–1456. https://doi.org/10.2337/diab.43.12.1450

Hill, M. A., & Larkins, R. G. (1989). Alterations in distribution of cardiac output in experimental diabetes in rats. *The American Journal of Physiology*, 257, H571–H580. https://doi.org/10.1152/ajpheart.1989.257.2.H571

Huynh, K., Bernardo, B. C., McMullen, J. R., & Ritchie, R. H. (2014). Diabetic cardiomyopathy: Mechanisms and new treatment strategies targeting antioxidant signaling pathways. *Pharmacology & Therapeutics*, 142, 375–415. https://doi.org/10.1016/j.pharmthera.2014.01.003

Jelinic, M., Conrad, K. P., Tare, M., & Parry, L. J. (2015). Differential effects of relaxin deficiency on vascular aging in arteries of male mice. *AGE (Dordrecht)*, 37(4), 1–12. https://doi.org/10.1007/s11357-015-9803-z

Jelinic, M., Leo, C. H., Marshall, S. A., Senadheera, S. N., Parry, L. J., & Tare, M. (2017). Short-term (48 hours) intravenous serelaxin infusion has no effect on myogenic tone or vascular remodeling in rat mesenteric arteries. *Microcirculation*, 24. https://doi.org/10.1111/micc.12371

Jelinic, M., Leo, C. H., Post Uiterweer, E. D., Sandow, S. L., Gooi, J. H., Wlodek, M. E., ... Parry, L. J. (2014). Localization of relaxin receptors in arteries and veins, and region-specific increases in compliance and bradykinin-mediated relaxation after in vivo serelaxin treatment. *The FASEB Journal*, 28, 275–287. https://doi.org/10.1096/fj.13-233429

Kahlberg, N., Qin, C. X., Anthonisz, J., Jap, E., Ng, H. H., Jelinic, M., ... Leo, C. H. (2016). Adverse vascular remodelling is more sensitive than endothelial dysfunction to hyperglycaemia in diabetic rat mesenteric arteries. *Pharmacological Research*, 111, 325–335. https://doi.org/10.1016/j.phrs.2016.06.025

Kilkenny, C., Browne, W., Cuthill, I. C., Emerson, M., & Altman, D. G. (2010). Animal research: Reporting *in vivo* experiments: The ARRIVE guidelines. *British Journal of Pharmacology*, 160, 1577–1579.

Koczulla, R., von Degenfeld, G., Kupatt, C., Krotz, F., Zahler, S., Gloe, T., ... Bals, R. (2003). An angiogenic role for the human peptide antibiotic LL-37/hCAP-18. *The Journal of Clinical Investigation*, 111, 1665–1672. https://doi.org/10.1172/JCI17545

Kusters, D. H., Chatrou, M. L., Willems, B. A., De Saint-Hubert, M., Bauwens, M., van der Vorst, E., ... Reutingsperger, C. P. (2015). Pharmacological treatment with Annexin A1 reduces atherosclerotic plaque burden in $LDLR^{-/-}$ mice on western type diet. *PLoS ONE*, 10, e0130484. https://doi.org/10.1371/journal.pone.0130484

Leo, C. H., Jelinic, M., Gooi, J. H., Tare, M., & Parry, L. J. (2014). A vasoactive role for endogenous relaxin in mesenteric arteries of male mice. *PLoS ONE*, 9, 1–12.

Marshall, S. A., Ng, L., Unemori, E. N., Girling, J. E., & Parry, L. J. (2016). Relaxin deficiency results in increased expression of angiogenesis- and remodelling-related genes in the uterus of early pregnant mice but does not affect endometrial angiogenesis prior to implantation. *Reproductive Biology and Endocrinology*, 14, 11. https://doi.org/10.1186/s12958-016-0148-y

Martinez-Lemus, L. A., Hill, M. A., & Meininger, G. A. (2009). The plastic nature of the vascular wall: A continuum of remodeling events contributing to control of arteriolar diameter and structure. *Physiology*, 24, 45–57. https://doi.org/10.1152/physiol.00029.2008

Mukherjee, B., Hossain, C. M., Mondal, L., Paul, P., & Ghosh, M. K. (2013). Obesity and insulin resistance: An abridged molecular correlation. *Lipid Insights*, 6, 1–11. https://doi.org/10.4137/LPI.S10805

Ng, H. H., Leo, C. H., Prakoso, D., Qin, C., Ritchie, R. H., & Parry, L. J. (2017). Serelaxin treatment reverses vascular dysfunction and left ventricular hypertrophy in a mouse model of Type 1 diabetes. *Scientific Reports*, 7, 39604. https://doi.org/10.1038/srep39604

Ohnishi, M., Tokuda, M., Masaki, T., Fujimura, T., Tai, Y., Itano, T., ... Takahara, J. (1995). Involvement of annexin-I in glucose-induced insulin secretion in rat pancreatic islets. *Endocrinology*, 136, 2421–2426. https://doi.org/10.1210/endo.136.6.7750463

Pan, B., Kong, J., Jin, J., Kong, J., He, Y., Dong, S., ... Zheng, L. (2016). A novel anti-inflammatory mechanism of high density lipoprotein through up-regulating annexin A1 in vascular endothelial cells. *(BBA)-Molecular Cell Biology of Lipids*, 1861, 501–512. https://doi.org/10.1016/j.bbalip.2016.03.022

Paravicini, T. M., Yogi, A., Mazur, A., & Touyz, R. M. (2009). Dysregulation of vascular TRPM7 and annexin-1 is associated with endothelial dysfunction in inherited hypomagnesemia. *Hypertension*, 53, 423–429. https://doi.org/10.1161/HYPERTENSIONAHA.108.124651

Perretti, M., & D'Acquisto, F. (2009). Annexin A1 and glucocorticoids as effectors of the resolution of inflammation. *Nature Reviews Immunology*, 9, 62–70. https://doi.org/10.1038/nri2470

Perretti, M., & Dalli, J. (2009). Exploiting the annexin A1 pathway for the development of novel anti-inflammatory therapeutics. *British Journal of Pharmacology*, 158, 936–946. https://doi.org/10.1111/j.1476-5381.2009.00483.x

Pourageaud, F., & De Mey, J. G. R. (1997). Structural properties of rat mesenteric small arteries after 4-wk exposure to elevated or reduced blood flow. *The American Journal of Physiology*, 273, H1699–H1706. https://doi.org/10.1152/ajpheart.1997.273.4.H1699

Prenner, S. B., & Chirinos, J. A. (2015). Arterial stiffness in diabetes mellitus. *Atherosclerosis*, 238, 370–379. https://doi.org/10.1016/j.atherosclerosis.2014.12.023

Purvis, G. S. D., Chiazza, F., Chen, J., Azevedo-Loiola, R., Martin, L., Kusters, D. H. M., ... Solito, E. (2018). Annexin A1 attenuates microvascular complications through restoration of Akt signalling in a murine model of type 1 diabetes. *Diabetologia*, 61, 482–495. https://doi.org/10.1007/s00125-017-4469-y

Purvis, G. S. D., Collino, M., Loiola, R. A., Baragetti, A., Chiazza, F., Brovelli, M., ... Thiemermann, C. (2019). Identification of AnnexinA1 as an endogenous regulator of RhoA, and its role in the pathophysiology and experimental therapy of type 2 diabetes. *Frontiers in Immunology*, 10, 571. https://doi.org/10.3389/fimmu.2019.00571

Qin, C. X., Buxton, K. D., Pepe, S., Cao, A. H., Venardos, K., Love, J. E., ... Ritchie, R. H. (2013). Reperfusion-induced myocardial dysfunction is prevented by endogenous annexin-A1 and its N-terminal-derived peptide Ac-ANX-A1(2-26). *British Journal of Pharmacology*, 168, 238–252. https://doi.org/10.1111/j.1476-5381.2012.02176.x

Qin, C. X., Rosli, S., Deo, M., Cao, N., Walsh, J., Tate, M., ... Ritchie, R. H. (2019). Cardioprotective Actions of the Annexin-A1 N-Terminal

Peptide, Ac2-26, Against Myocardial Infarction. *Frontiers in Pharmacology*, 10, 269. https://doi.org/10.3389/fphar.2019.00269

Qin, C. X., Yang, Y. H., May, L., Gao, X., Stewart, A. G., Tu, Y., … Ritchie, R. H. (2015). Cardioprotective potential of annexin-A1 mimetics in myocardial infarction. *Pharmacology & Therapeutics*, 148, 47–65. https://doi.org/10.1016/j.pharmthera.2014.11.012

Rackham, C. L., Vargas, A. E., Hawkes, R. G., Amisten, S., Persaud, S. J., Austin, A. L., … Jones, P. M. (2016). Annexin A1 is a key modulator of mesenchymal stromal cell-mediated improvements in islet function. *Diabetes*, 65, 129–139. https://doi.org/10.2337/db15-0990

Raskin, P., & Mohan, A. (2010). Emerging treatments for the prevention of type 1 diabetes. *Expert Opinion on Emerging Drugs*, 15, 225–236. https://doi.org/10.1517/14728211003694631

Ritchie, R. H., Gordon, J. M., Woodman, O. L., Cao, A. H., & Dusting, G. J. (2005). Annexin-1 peptide Anx-1(2-26) protects adult rat cardiac myocytes from cellular injury induced by simulated ischaemia. *British Journal of Pharmacology*, 145, 495–502.

Ritchie, R. H., Love, J. E., Huynh, K., Bernardo, B. C., Henstridge, D. C., Kiriazis, H., … McMullen, J. R. (2012). Enhanced phosphoinositide 3-kinase(p110α) activity prevents diabetes-induced cardiomyopathy and superoxide generation in a mouse model of diabetes. *Diabetologia*, 55, 3369–3381. https://doi.org/10.1007/s00125-012-2720-0

Ritchie, R. H., Sun, X., Bilszta, J. L., Gulluyan, L. M., & Dusting, G. J. (2003). Cardioprotective actions of an N-terminal fragment of annexin-1 in rat myocardium in vitro. *European Journal Pharmacology*, 461, 171–179. https://doi.org/10.1016/S0014-2999(03)01314-1

Santana, A. B. C., de Souza Oliveira, T. C., Bianconi, B. L., Barauna, V. G., Santos, E. W. C. O., Alves, T. P., & Krieger, J. E. (2014). Effect of high-fat diet upon inflammatory markers and aortic stiffening in mice. *Biomed Res Intl*, 2014, 914102.

Sasson, A. N., & Cherney, D. Z. (2012). Renal hyperfiltration related to diabetes mellitus and obesity in human disease. *World Journal of Diabetes*, 3, 1–6. https://doi.org/10.4239/wjd.v3.i1.1

Schalkwijk, C. G., Poland, D. C., van Dijk, W., Kok, A., Emeis, J. J., Dräger, A. M., … Stehouwer, C. D. A. (1999). Plasma concentration of C-reactive protein is increased in type I diabetic patients without clinical macroangiopathy and correlates with markers of endothelial dysfunction: evidence for chronic inflammation. *Diabetologia*, 42, 351–357. https://doi.org/10.1007/s001250051162

Souza-Smith, F. M., Katz, P. S., Trask, A. T., Stewart, J. A., Lord, K. C., Varner, K. J., … Lucchesi, P. A. (2011). Mesenteric resistance arteries in type 2 diabetic db/db mice undergo outward remodeling. *PLoS ONE, 6*, e23337. https://doi.org/10.1371/journal.pone.0023337

Stehouwer, C. D. A., Henry, R. M. A., & Ferreira, I. (2008). Arterial stiffness in diabetes and the metabolic syndrome: A pathway to cardiovascular disease. *Diabetologia*, 51, 527–539. https://doi.org/10.1007/s00125-007-0918-3

Unthank, J. L., & Bohlen, H. G. (1987). Quantification of intestinal microvascular growth during maturation: Techniques and observations. *Circulation Research*, 61, 616–624. https://doi.org/10.1161/01.res.61.5.616

Wigg, S. J., Tare, M., Forbes, J., Cooper, M. E., Thomas, M. C., Coleman, H. A., … O'Brien, R. C. (2004). Early vitamin E supplementation attenuates diabetes-associated vascular dysfunction and the rise in protein kinase C-β in mesenteric artery and ameliorates wall stiffness in femoral artery of Wistar rats. *Diabetologia*, 47, 1038–1046. https://doi.org/10.1007/s00125-004-1411-x

Wilkinson, I. B., Westerbacka, J., Yki-Jarvinen, H., & Cockcroft, J. R. (2001). Diabetes and arterial stiffness. In M. T. Johnstone, & A. Veves (Eds.), *Diabetes and cardiovascular disease* (pp. 343–360). Totowa, New Jersey: Humana Press. https://doi.org/10.1385/1-59259-091-8:343

Yang, Y. H., Morand, E. F., Getting, S. J., Paul-Clark, M., Liu, D. L., Yona, S., … Flower, R. J. (2004). Modulation of inflammation and response to dexamethasone by Annexin 1 in antigen-induced arthritis. *Arthritis and Rheumatism*, 50, 976–984. https://doi.org/10.1002/art.20201

Zieman, S. J., Melenovsky, V., & Kass, D. A. (2005). Mechanisms, pathophysiology and therapy of arterial stiffness. *Arteriosclerosis, Thrombosis, and Vascular Biology*, 25, 932–943. https://doi.org/10.1161/01.ATV.0000160548.78317.29

Zimmet, P., Alberti, K. G., & Shaw, J. (2001). Global and societal implications of the diabetes epidemic. *Nature, 414*, 782–787. https://doi.org/10.1038/414782a